



## Generic dynamic model of rechargeable batteries



R.H. Milocco<sup>a,\*</sup>, J.E. Thomas<sup>b</sup>, B.E. Castro<sup>b</sup>

<sup>a</sup> Grupo Control Automático y Sistemas (GCAyS), Depto. Electrotecnia, Facultad de Ingeniería, Universidad Nacional del Comahue, Buenos Aires 1400, 8300 Neuquén, Argentina

<sup>b</sup> Instituto de Investigaciones Físicoquímicas Teóricas y Aplicadas (INIFTA), UNLP, CCT La Plata-CONICET, CC 16, Suc. 4, 1900 La Plata, Argentina

### HIGHLIGHTS

- We model rechargeable batteries for use in BMS design.
- The rate capacity effect and the state of charge are explicitly considered.
- The model is based on an electrochemical approach.
- A reduced-order model with electrochemical sense is presented.
- This approach is able to interpret the most commonly used models in the literature.

### ARTICLE INFO

#### Article history:

Received 15 June 2013

Received in revised form

27 July 2013

Accepted 1 August 2013

Available online 14 August 2013

#### Keywords:

Battery model

Rate capacity

State of charge

Wiener model

Energy storage model

### ABSTRACT

There are numerous models of rechargeable batteries in the current literature. Some of them are complicated electrochemical approaches; others, are given by simple analogies. However, simple models with electrochemical states capable of describing important quantities, like the rate capacity effect and the recovery effect, are hard to find. In this paper, based on an electrochemical approach, we present a generalized model suitable for use in BMS applications, which takes into account explicitly the rate capacity effect and the state of charge. Moreover, the model is thought up for general energy storage processes based on mass transport and charge transfer. The proposed general model approach is able to interpret the most commonly used models in the literature.

© 2013 Elsevier B.V. All rights reserved.

### 1. Introduction

The battery model is necessary both for estimation and prediction, which are very important topics for battery management systems (BMS). A good model is needed in order to know the on-line state of charge (SOC), the state of health (SOH), and the available power, also to decide control actions for equalization and for battery pack design. An important feature of rechargeable batteries is that the voltage drops faster for high discharge currents. Thereby, the effective capacity drops for high discharge rates. This effect is called rate capacity effect (RCE) and it is associated with the recovery effect (RE), which is the time required for battery recuperation. Both quantities are important for an optimal use of batteries.

In the current literature there are numerous models of rechargeable batteries. Some of them are complicated electrochemical approaches; others, are given by simple analogies. However, it is difficult to find practical models that interpret the RCE and the RE using electrochemical states. In this paper, based on an electrochemical approach, we present a generalized model, suitable for use in BMS applications, which takes into account explicitly the RCE and the RE. The novel contribution is that our model has a simple structure composed by the cascaded of a pure integrator, a high pass-filter (HPF), and a nonlinear function; all these components related with explicit important electrochemical states, like SOC, and surface charge concentration, which is a key variable for describing the concepts of RCE and RE. Moreover, the model is proposed for general energy storage processes based on mass transport and charge transfer. This approach is able to interpret the most commonly used models in the literature.

The development of an accurate dynamic battery model is difficult due to the nonlinear infinite-dimensional and distributed

\* Corresponding author. Tel./fax: +54 299 4488305.

E-mail addresses: [rmilocco@yahoo.com.ar](mailto:rmilocco@yahoo.com.ar), [ruben.milocco@fain.uncoma.edu.ar](mailto:ruben.milocco@fain.uncoma.edu.ar) (R.H. Milocco), [enryjt@inifta.unlp.edu.ar](mailto:enryjt@inifta.unlp.edu.ar) (J.E. Thomas), [bcastro@inifta.unlp.edu.ar](mailto:bcastro@inifta.unlp.edu.ar) (B.E. Castro).

mass transport processes governing electrochemical system dynamics. Physiochemical models provide an accurate insight on battery processes, but models based on fundamental physiochemical principles are rarely employed in real time, due to their high order and computational requirements. The need to identify a great number of parameters is also a drawback. Several kinds of simplifications have been presented in some publications; for example, diffusion limitations in the electrolyte and potential distribution in the porous structure of the electrodes are disregarded in Ref. [1]. Other models are focused on the simplification of the diffusion dynamics in the active material. In this direction, in Ref. [2] a second degree polynomial approximation is used to model the concentration profile in the active material. Barbarisi [3] presents a Ni-MH electrochemical model driven by the measured current and potential. For this model several kinetic and transport parameters of the battery, which are difficult to obtain, need to be known. In order to overcome this difficulty, the static nonlinearity can be approximated by using a Taylor series expansion and by identifying the coefficient applying linear regression, as in Ref. [4]. In recent publications [5–7] reduced order models based on frequency domain transfer function analysis, are presented.

A widely used approach to model batteries consists in employing analogies with electrical circuits where the voltage source is the open circuit voltage (OCV). The analogies with electrical circuits are presented in Refs. [8,9] as well as the references they contain. These models have been extensively used, for example in Ref. [10], to estimate the SOC in a Lithium Polymer battery with nonlinear sliding observers; in Ref. [11], for hybrid electric vehicles with lead acid batteries; in Ref. [12], with nonlinear observers to estimate the parameters of the model and the SOC jointly; also in Ref. [13], to estimate the SOC in lead acid batteries. Such models are simple, but difficult to relate with the battery chemical states. One well-known model used to represent the dynamics of the stored charge for design engineering applications was presented in Ref. [14]. It is a battery model based on the approach of chemical kinetics, known as *kinetic battery model*. Specifically, it takes into account the rate capacity effect by assuming that the charge can be stored in two ways, either as immediately available or as chemically bound. Although this model interprets the RCE, is not able to represent the output voltage as a natural function of electrochemical states requiring special adjustments based on tables.

Basically, simple analogies are practical but empirical and sometimes they do not work properly. On the other extreme, there are electrochemical models with several parameters and states, which are very difficult to obtain. In this paper, following electrochemical arguments, we show that any rechargeable battery can be modeled as a cascade of a linear dynamic system with a static nonlinearity in a setup called Wiener model. The linear dynamic system is related to the transport of the reacting substances in the active material. These processes are governed by Fick's law and can be represented as a series of two subsystems; one is a pure integrator representing the real stored charge or SOC, and the other is a high-pass filter representing the dynamic of the concentration at the electrode interface and related to the rate capacity of the battery. The static nonlinearity is due to the electrochemical reactions at the electrode interfaces, and it is governed by a Butler–Volmer type equation but can also be combined with other reaction types described by a non-linear function which characterizes the electromotive force of the battery.

The paper is organized as follows: in Section 2 we present the model formulation basically through two main stages. First, the charge transfer process at the interface; and second, the diffusional process. In this section, the diffusional process is shown to be composed by two parts: one, a pure integrator, and the other a HPF.

The general model is presented in this section. In Section 3, the rate capacity effect is related to the diffusional process. In Section 4, we present a reduced order approximation and it is shown that in the case of second order approximation, the dynamics of diffusion follow the kinetic battery model. Connections with the Thevenin electrical circuit analogy are also presented. In Section 5, a procedure to identify the parameters together with experimental results are shown for different battery types, like Li-Ion, Ni-MH, and Lead Acid. Finally, we discuss the conclusions in Section 6.

## 2. Model formulation

A battery is basically a system conformed by two electrodes immersed in an electrolytic media. During discharge, the negative electrode is oxidized, while the positive electrode is reduced. The process is reversed during charge, being this global process responsible for energy storage or release. Battery electrodes are generally porous structures composed of particles of active material, conductive additives and adequate binders, supported on a conductive substrate acting as current collector, the whole assembly being immersed in the electrolytic media. Models for porous electrodes mainly use the porous electrode theory, as reviewed by Newman and Tiedemann [17]. In according to this theory, the liquid and the solid phases are approximated as superimposed continua. The intimate contact between both phases generates the interfacial surface, where the different electrochemical processes take place (electrochemical interface). In the energy storage or release processes, two main stages must be distinguished: one, corresponding to the charge transfer process at the electrodes electrochemical interface, including electrochemical reactions and double layer charging; and another one, corresponding to mass transfer, either in the electrolyte or in the electrode active material. In the next subsections, we describe both stages, which are the main part of our battery model.

### 2.1. Faradaic charge transfer processes

The electrochemical reactions taking place at the electrochemical interface give rise to the faradaic current,  $I(t)$ . The faradaic current may be described in terms of the Butler–Volmer equation, as follows [18,19]:

$$I = \tilde{k}^o e^{\alpha^o E} \left( \prod c_i^o \right) + \tilde{k}^r e^{\alpha^r E} \left( \prod c_i^r \right), \quad (1)$$

where  $\tilde{k}^r$  and  $\tilde{k}^o$  are constants corresponding to reduction and oxidation reactions;  $E$  is the electrode potential;  $\alpha^r = a^r F/RT$  and  $\alpha^o = a^o F/RT$  are constant with  $a^r = a^o - 1$  and  $a^o$  is a symmetry factor in the interval (0,1);  $F$  is the Faraday constant;  $R$  the universal gas constant;  $T$  is the temperature; and  $c_i^r$  and  $c_i^o$  are the concentration of reactants and products at the electrochemical interface. In the sequel we shall consider that the very high concentrations of species are constants, so for most batteries it is possible to reduce the complexity to a simple redox reaction, as follows [18,20]:

$$I = \tilde{k}^o c^o e^{\alpha^o E} - \tilde{k}^r c^r e^{\alpha^r E}. \quad (2)$$

By multiplying and dividing the first term on the right by  $\bar{c}^o$ , and by  $\bar{c}^r$  the second, which are the maximum concentration of the oxidized and reduced states of the active materials, the following simple equation holds:

$$I = k^o X^o e^{\alpha^o E} - k^r X^r e^{\alpha^r E}, \quad (3)$$

where  $k^r = \tilde{k}^r \bar{c}^r$  and  $k^o = \tilde{k}^o \bar{c}^o$  are constants, and  $X^r = c^r / \bar{c}^r$  and  $X^o = c^o / \bar{c}^o$  are the normalized concentrations at the interface, with

respect to the maximum concentration. Taking into account that concentration lies in the interval [0–1], it follows that each electrode fulfills  $X^r = 1 - X^o$ . In what follows, for notation simplicity, we neglect the superfix  $o$  by calling  $X = X^o$ ,  $c = c^o$ , and  $\bar{c} = \bar{c}^o$ . Then, equation (3) can be written as

$$I = f_I(E, X) = k^o X e^{\alpha^o E} - k^r (1 - X) e^{\alpha^r E}, \quad (4)$$

where  $f_I(E, X)$  is the Butler–Volmer equation expressing the functional relationship of current with respect to potential and concentration. From equation (4) it is possible to obtain the concentration at the electrode surface  $X$  explicitly, as

$$X = f_X(E, I) = \frac{k^r e^{\alpha^r E} + I}{k^r e^{\alpha^r E} + k^o e^{\alpha^o E}}. \quad (5)$$

Note that concentration  $X$  increases when the current that enter to the electrode is considered positive. Although it is not possible to obtain an explicit expression of the form  $E = f_E(I, X)$  from equation (5), in the Appendix A it is demonstrated that such function exists. It is important to note that when the faradaic current is zero, ( $I = 0$ ), by using logarithms in equation (5), the potential can be obtained explicitly as

$$E = f_E(0, X) = \frac{1}{\alpha^r - \alpha^o} \left( \log\left(\frac{X}{1 - X}\right) - \log\left(\frac{k^r}{k^o}\right) \right), \quad (6)$$

which is called Electro-Motive-Force (EMF). The battery EMF is denoted as  $E = f_E(0, X)$ , which represents the functional relationship of the potential with respect to the concentration  $X$  at zero current,  $I = 0$ . Note that the potential  $E$  increases when the concentration  $X$  increases.

It is worth noting that the potential at the electrode surface,  $E(t)$ , can be decomposed into a sum of two terms. One, is the equilibrium potential, defined by zero current,  $I = 0$ , and concentration  $X_{eq} = 0.5$ , denoted as  $E_0$  and is obtained using equation (6). The other, is the potential that depends on both the current and the concentration.

### 2.2. The diffusion process

The reacting substance approximates the electrode surface by diffusion. The second part of the model deals with the dynamics of the mass transport process, which determines the concentration  $X(t)$  described in equation (5). These are essentially diffusion processes, either in the electrolyte or in the electrode active materials. The number of substance moles that reacts at the electrochemical interface is proportional to the electrons produced or consumed, according to the Faraday constant. The electrons flow through the load while the reacting substance is accumulated. The total amount of such moles is proportional to the accumulated amount of charge giving the SOC of the battery, as follows:

$$SOC(t) = \frac{1}{Q_{max}} \left( Q_0 + \int_0^t I(\tau) d\tau \right), \quad (7)$$

where  $Q_0$  and  $Q_{max}$  are the initial and the maximum battery charge. The quantity  $Q_{max}$  is called battery capacity and is defined as the product of a very low constant current multiplied by the time required to reach the maximum charge, starting with the battery completely discharged ( $Q_0 = 0$ ).

In order to model the diffusional process, consider that the reacting substance is accumulated or released by diffusion from an area of higher concentration to another of lower one. Assume that the physical place where the reacting mass is stored is divided into

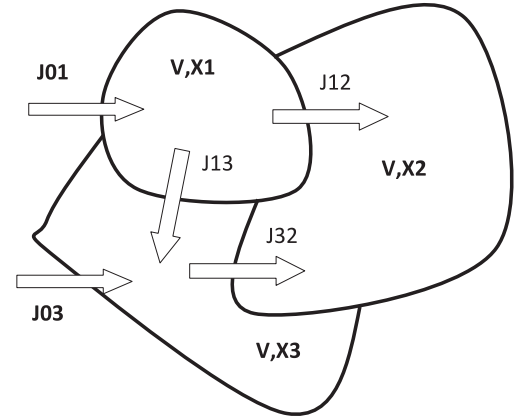


Fig. 1. Example of storage matter by diffusion. Compartments 1 and 3 are in contact with the electrolyte.

$N$  small volumes, each with volume ( $V$ ) equal to each other, with constant fractional concentrations denoted as  $x_i$  for  $i = 1, \dots, N$ . Then, by denoting the mass flow as  $J_{ij}$ , in mass/time units, from compartments  $i$  to  $j$ , the following relationships,  $\forall j \neq i$ , hold:

$$J_{ij} = K_{ij}(x_i - x_j), \quad (8)$$

$$K_{ji} = K_{ij} \quad (9)$$

$$J_{ij} = -J_{ji}; \quad (10)$$

where  $K_{ij}$  is in mass/time units; suffix  $I = 0$  corresponds to the differential compartments adjacent to the contact surface with the electrolyte, the interface. There is also an associated mass balance, which is given by

$$\frac{dx_i}{dt} = -\gamma \sum_{j=1, N} J_{ij}, \quad (11)$$

with  $\gamma = 1/V\tau$  in 1/mass units, and

$$\sum_{j=1, M} J_{0j} = \frac{I}{F}, \quad (12)$$

where  $M$  is the number of compartments adjacent to the surface in contact with the electrolyte. The state of charge is the total accumulated charge and it is given by

$$SOC(t) = \sum_{i=1, N} \frac{x_i(t)}{N}. \quad (13)$$

A simple example of three compartments will be shown for clarity. Assume that the material, where the mass is stored, has  $N = 3$  with  $M = 2$  compartments, as it is shown in Fig. 1. Then, the mass balance equations are given by

$$\begin{aligned} \dot{x}_1 &= \gamma(J_{01} - J_{12} - J_{13}), \\ \dot{x}_2 &= \gamma(J_{12} + J_{32}), \\ \dot{x}_3 &= \gamma(J_{03} + J_{13} - J_{32}), \end{aligned}$$

where

$$\begin{aligned} J_{12} &= K_{12}(x_1 - x_2), \\ J_{13} &= K_{13}(x_1 - x_3), \\ J_{32} &= K_{32}(x_3 - x_2). \end{aligned} \quad (14)$$

$J_{01}$  and  $J_{03}$  are inputs. Taking into account that  $K_{ij} = K_{ji}$ , and defining  $a_1$  and  $a_3$  as the fractional part of the sum of incoming mass flow  $J^t = J_{01} + J_{03}$ , such that  $a_1 + a_3 = 1$ , the following holds:

$$J_{01} = a_1 J^t; \quad J_{03} = a_3 J^t. \tag{15}$$

The system equations can be written in a matrix form by

$$\dot{\mathbf{x}}(t) = \mathbf{A}\mathbf{x}(t) + \gamma \mathbf{B}J^t, \tag{16}$$

where

$$\mathbf{x}(t) = [x_1, x_2, x_3]^T; \quad \mathbf{B} = [a_1, 0, a_3]^T$$

$$\mathbf{A} = \gamma \begin{pmatrix} -K_{12} - K_{13} & K_{12} & K_{13} \\ K_{12} & -K_{32} - K_{12} & K_{32} \\ K_{13} & K_{32} & -K_{32} - K_{13} \end{pmatrix}.$$

We are interested in obtaining the dynamical relationship between the charge current and the concentration at the interface  $X$ . To this end, let us average the individual concentrations corresponding to the  $M$  differential volumes, at the interface, in contact with the electrode surface. This is obtained by multiplying  $\mathbf{B}^T$  by the vector  $\mathbf{x}$ , as follows:

$$X = \mathbf{B}^T \mathbf{x}(t). \tag{17}$$

The transfer function between concentration and charge current is obtained from this definitions by applying the Laplace transform to equations (16) and (17) resulting in the following input/output relationship:

$$\mathcal{X}(S) = H(S)\mathcal{I}(S), \tag{18}$$

where  $\mathcal{X}(S)$  and  $\mathcal{I}(S)$  are the Laplace transform of  $X$  and  $I$ ;  $S$  is a complex variable, and

$$H(S) = \mathbf{B}^T (S\mathbb{I} - \mathbf{A})^{-1} \mathbf{B} \gamma / F, \tag{19}$$

where  $\mathbb{I}$  means identity matrix. Before continuing, it is important to say that the same procedure can be extended to the case of  $N$  constant volume partitions, as follows:

$$\mathbf{x}(t) = [x_1, x_2, \dots, x_N]^T; \quad J^t = \sum_{i=1}^M J_{0i};$$

$$\mathbf{A} = \begin{pmatrix} -\sum_{j=1, N} K_{1j} & K_{12} & K_{13} & \dots & K_{1N} \\ K_{21} & -\sum_{j=1, N} K_{2j} & K_{23} & \dots & K_{2N} \\ \dots & \dots & \dots & \dots & \dots \\ K_{N1} & K_{N2} & \dots & K_{N3} & -\sum_{j=1, N} K_{Nj} \end{pmatrix}, \tag{20}$$

where  $J_{0i}$  represents the mass flow that enter to each of the  $M$  compartments in contact with the surface, and  $\mathbf{B}$  is a column vector having a constant entry value  $a_i$  if the infinitesimal volume  $V$  is in contact with the surface and zero otherwise. The  $M$  constants  $a_i$  are constrained to  $\sum_{i=1, M} a_i = 1$ . The total mass flow generated by the reacting substances at the surface of the electrode is  $J^t = \sum_{i=1, M} J_{0i} = \sum_{i=1, M} a_i J^t$ . Note that ideally, the expanded matrices  $\mathbf{A}$ ,  $\mathbf{B}$ , and  $\mathbf{C}$  are infinite-dimensional, but still can be used in equations (17)–(19), obtaining an infinite-dimensional-linear dynamic system.

By multiplying and dividing equation (18) by  $SQ_{\max}$ , the functional relationship between the current and the concentration at the interface can be rewritten as a function of the state of charge as

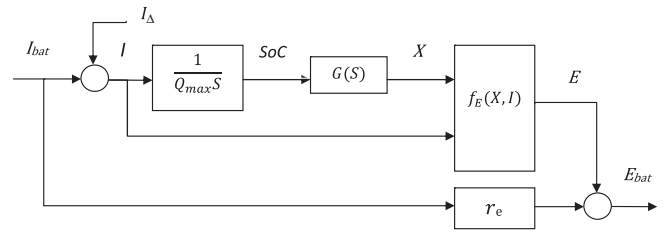


Fig. 2. Battery model.

$$\mathcal{X}(S) = G(S)\text{SOC}(S), \tag{21}$$

where

$$G(S) = H(S)SQ_{\max}; \tag{22}$$

$$\text{SOC}(S) = \frac{\mathcal{I}(S)}{SQ_{\max}}. \tag{23}$$

### 2.3. The complete model

It should be noted that the battery is formed by two electrode–electrolyte interfaces. However, since generally only one is limiting, it is possible to represent the global dynamics with only one equivalent electrode. Apart from diffusion and static nonlinearity, the complete battery model should include the electrolyte ohmic resistance ( $r_e$ ) and the effect of the double layer capacity ( $C_{dl}$ ). The complete model is obtained by relating the charge transfer  $E = f_E(I, X)$ , the diffusion processes (21),  $r_e$ , and the current ( $I_\Delta$ ), which includes the current due to the capacity of double layer and others derived from secondary reactions such that  $I_{\text{bat}} = I + I_\Delta$ , where  $I_{\text{bat}}$  is the current measured at the battery terminals. Thus, the rechargeable battery can be modeled as a cascade of a linear dynamic system followed by a static nonlinearity, as shown in Fig. 2, which is known as the *Wiener model* [4].

### 3. The rate capacity effect

Since the redox reaction occurs at the electrode surface and that the charge transport process is diffusive, for a given charge/discharge current,  $X$  increases/decreases faster than the SOC. By taking into account that  $E$  depends directly on  $X$ , the useful capacity of the battery heavily depends on the charge/discharge current profile. Great current demands reduce the effective capacity of the battery. This effect is reflected on the high-rate discharge behavior of the battery and it is called *rate capacity effect* (RCE), [15], and it is important for battery use optimization, [16]. It can be seen from equation (21) that  $X$  and SOC are related by the dynamics imposed by the filter  $G(S)$ , which determines the rate capacity  $H(S)$  of the battery and also the recovery time. Thus, we are interested in studying the filtering properties of  $G(S)$ .

First, note that  $G(S)$  is an infinite dimensional rational function in the variable  $S$ . Secondly, its steady state gain is equal to one. To prove the last, note that in steady state the mass is equally distributed in all the small volumes, and by considering that both the SOC and the fractional  $X$  are in the interval  $[0,1]$ , it follows that in steady state both quantities are equal. Thus, from equation (21), it means that the steady state gain of  $G(S)$  is equal to one,  $G(0) = 1$ . Now we will show that  $G(j\omega)$  is an infinite dimensional rational HPF. To this end, let us define a positive real function and two important properties.

A rational function  $H(S)$  is called positive real function – PRF – if and only if  $H(S)$  is real when  $S$  is real, and  $\text{Re}(H(S)) \geq 0$  when  $\text{Re}(S) \geq 0$ , see Ref. [21] for details. If  $H(S)$  is a PRF, it is called impedance and the following properties hold: i) the absolute value of the phase angle of  $H(S)$  is never greater than  $\pi/2$ ; ii)  $H(S)$  cannot have any poles or zeros in the right-half  $S$ -plane, i.e. it is a minimum phase system. In the Appendix B it is shown that  $H(S)$  in equation (18) is a PRF. Then, because  $H(S)$  is a cascade of a pure integrator element and the filter  $G(S)$ , it is clear that in order to fulfill the property i, the element  $G(S)$  must have a positive phase. From the property ii, and taking into account the foregoing, the module must necessarily be greater than, or equal to, unity. Given that low-frequency gain is unity, the filter frequency response of  $G(j\omega)$  necessarily amplifies high frequencies. Thus,  $G(j\omega)$  is a HPF.

As an example, consider the case where a planar diffusion process is governed by Fick’s law, which is a very good approximation for some batteries. The Laplace transform of concentration  $\mathcal{X}(S)$  is derived in Ref. [22]. In the case of finite diffusion and impermeable barrier, it has the following expression:

$$\mathcal{X}(S) = \frac{L \coth \varphi(S)}{\text{FAD} \varphi(S)} \mathcal{I}(S), \tag{24}$$

where  $D$  is the diffusion constant,  $L$  and  $A$  are the thickness depth and the area of the electrode, and  $\varphi(S) = L\sqrt{S/D}$ . Multiplying and dividing by  $\varphi(S)$  the expression can be rewritten as

$$\mathcal{X} = \frac{\mathcal{I}(S)}{Q_{\max} S} G(S), \tag{25}$$

where  $Q_{\max} = 1/FV$  with volume  $V = AL$  and

$$G(S) = \varphi \coth \varphi, \tag{26}$$

The frequency response  $G(S = j\omega)$  corresponds to a linear infinite dimensional HPF, unity static gain, with frequency response as shown in Fig. 3. A similar analysis can be made for spherical diffusional processes. In such cases, the concentration has the following Laplace transform:

$$\mathcal{X}(S) = \frac{L \tanh \varphi(S)}{\text{FAD} (\tanh \varphi(S) - \varphi(S))} \mathcal{I}(S), \tag{27}$$

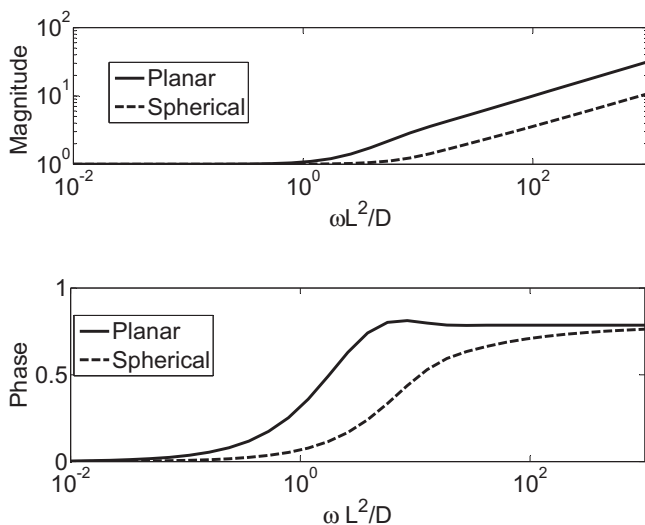


Fig. 3. Frequency response of filter  $G(j\omega)$  for planar diffusion symmetry in solid electrode.

where  $L$  is now the radio and  $A$ , the area of the sphere. By considering that the volume of the sphere is  $V = AL/3$ , the equation can be written as equation (25), where  $G(S)$  is now given by

$$G(S) = \frac{\varphi^2(S)}{3} \frac{\tanh \varphi(S)}{(\tanh \varphi(S) - \varphi(S))}, \tag{28}$$

with frequency response also shown in Fig. 3. Note that, in both cases, the function admits infinite derivatives with respect to  $S$ . Thus, they can be written as an infinite dimensional rational HPF in  $S$ , as in equations (19), (20) and (22).

#### 4. A practical approximated model

As it was shown, the filter  $G(S)$  is an infinite dimensional linear system described by ordinary differential equations. However, in order to have a generalized working expression, we assume that a finite order can be used as a good approximation. The following unit gain  $n$ th-order rational function is used to approximate the infinite dimensional  $G(S)$ :

$$G(S) = \frac{N(S) + n_n S^n}{D(S)}, \tag{29}$$

where

$$\begin{aligned} N(S) &= d_0 + n_1 S + \dots + n_{n-1} S^{n-1} \\ D(S) &= d_0 + d_1 S + \dots + d_{n-1} S^{n-1} + S^n. \end{aligned}$$

Note that the HPF requires equal order for numerator and denominator polynomials and equal constant term  $d_0$ , for unit gain. By replacing the above in equation (21), the concentration can be written conveniently, for further parameter identification purposes, as the sum of two terms, one depending on SOC and the other, depending on  $I$ , as follows:

$$\mathcal{X}(S) = \frac{N(S)}{D(S)} \text{SOC}(S) + \frac{n_n S^{n-1}}{Q_{\max} D(S)} \mathcal{I}(S). \tag{30}$$

Any given transfer function which is strictly proper (denominator polynomial order greater than numerator polynomial order), can easily be transferred into state-space observable canonical form [32]. Then, a useful way to write the above equation, to be used in what follows, is in the time-domain as

$$\dot{\mathbf{x}}(t) = \Phi \mathbf{x}(t) + \Gamma_1 \text{SOC}(t) + \Gamma_2 I(t), \tag{31}$$

where

$$\begin{aligned} \Phi &= \begin{pmatrix} -d_{n-1} & 1 & 0 & 0 & \dots & 0 \\ \vdots & 0 & 1 & 0 & \dots & 0 \\ \vdots & \vdots & \ddots & \ddots & \ddots & 0 \\ -d_1 & 0 & 0 & 0 & \dots & 1 \\ -d_0 & 0 & 0 & 0 & \dots & 0 \end{pmatrix}; \Gamma_1 = \begin{pmatrix} n_{n-1} \\ \vdots \\ d_0 \end{pmatrix}; \\ \Gamma_2 &= \begin{pmatrix} n_n/Q_{\max} \\ 0 \\ \vdots \\ 0 \end{pmatrix}, \end{aligned}$$

and the concentration  $X(t)$  is given by

$$X(t) = C \mathbf{x}, \tag{32}$$

where  $C = [1, 0, \dots, 0]$ . Using the above, the complete model in state variables can be written as follows:

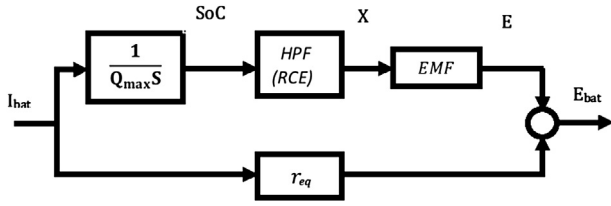


Fig. 4. Model approximation where HPF is the finite order unit gain high pass filter approximation of  $G(S)$  representing the rate capacity effect.

$$\begin{pmatrix} \dot{SOC}(t) \\ \dot{\mathbf{x}} \end{pmatrix} = \begin{pmatrix} 0 & | & 0 \\ \hline -\Gamma_1 & | & -\Phi \end{pmatrix} \begin{pmatrix} SOC(t) \\ \mathbf{x} \end{pmatrix} + \begin{pmatrix} 1/Q_{max} \\ \Gamma_2 \end{pmatrix} I_{bat}(t) + \chi \quad (33)$$

$$E_{bat}(t) = f_E(I, C\mathbf{x}) + r_{eq}I_{bat}(t), \quad (34)$$

where  $\chi$  is a disturbance vector to the states which includes the effect of current  $I_{\Delta}$  and other possible disturbances.  $E_{bat}$  is the potential at the battery terminals which include the electrode potential,  $E$ , plus the ohmic drop.

There are several approaches that can be used to choose the appropriate model order ( $n$ ). Statistical methods, such as the Akaike criterion, [33], or the robust approach used in Ref. [6]. The reduced order approximation of HPF together with a normalized basis for the nonlinear voltage equation, like polynomials, expansion of Taylor series, wavelets, radial basis functions, etc., could be used for identification of the Wiener model (33) and (34) (see Refs. [25,26]). However, a further approximation can be made by considering the voltage model as formed by the sum of two terms. One nonlinear that depends solely on the concentration and another linear, that depends only on the current:

$$E_{bat} = f_E(I, X) + r_{eq}I_{bat} \approx f_E(0, X) + r_{eq}I_{bat}, \quad (35)$$

where the equivalent resistance,  $r_{eq} = \partial E_{bat} / \partial I_{bat}$ , includes not only the resistance of the electrolyte, but also the resistance of the charge transfer. In Appendix C a formal expression of  $r_{eq}$  is given. Although the resistance due to charge transfer is dependent on both current and state of charge, it is considered constant.

It is important at this point to establish the relationship between EMF ( $f_E(0, X)$ ) and the OCV ( $f_E(0, SOC)$ ). The EMF is the function  $E = f_E(0, X)$  which relates the potential  $E$  with concentration  $X$  and the OCV is the same as EMF but considered in steady state. Since at steady state fulfills  $X = SOC$ , in such conditions, both EMF and OCV are the same. The final approximated model is depicted in Fig. 4, where the disturbance vector to the states  $\chi$  was neglected, consequently  $I = I_{bat}$  fulfills.

#### 4.1. The first order HPF approximation and its relationship with other known linear models

Considering a first order approximation of the high-pass filter in equation (33) and neglecting the disturbance vector  $\chi$ , we obtain the following second order model for diffusion:

$$\begin{pmatrix} \dot{SOC}(t) \\ \dot{X}(t) \end{pmatrix} = \begin{pmatrix} 0 & 0 \\ d_0 & -d_0 \end{pmatrix} \begin{pmatrix} SOC(t) \\ X(t) \end{pmatrix} + \begin{pmatrix} 1 \\ n_1 \end{pmatrix} \frac{I_{bat}(t)}{Q_{max}}. \quad (36)$$

In order to obtain a linear expression for the voltage equation, a further approximation can be made from equation (34) by linearizing the increments of the nonlinear term, as follows:

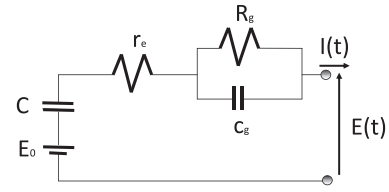


Fig. 5. Equivalent circuit for second order approximation.  $C = Q_{max}/\mu$ ,  $R_g = \mu(n_1 - 1)/d_0Q_{max}$  and  $C_g = Q_{max}/\mu(n_1 - 1)$ .

$$E_{bat} = f_E(0, X) + r_{eq}I_{bat} \approx E_0 + \mu X + r_{eq}I_{bat}, \quad (37)$$

where  $\mu$  and  $E_0$  are constants used for the pseudolinear approximation of the EMF. By using this pseudolinear model, it is possible to derive an analog electric circuit by performing the Laplace transform to equations (36) and (37), which gives

$$E_{bat}(S) = \begin{pmatrix} 0 & \mu \end{pmatrix} \left( S\mathbb{I} - \begin{pmatrix} 0 & 0 \\ d_0 & -d_0 \end{pmatrix} \right)^{-1} \begin{pmatrix} 1 \\ n_1 \end{pmatrix} \frac{I_{bat}(S)}{Q_{max}} + E_0 + r_{eq}I_{bat}(S) \quad (38)$$

$$E_{bat}(S) = \left( \frac{\mu}{SQ_{max}} + \frac{\mu(n_1 - 1)}{(d_0 + S)Q_{max}} + r_{eq} \right) I_{bat}(S) + E_0. \quad (39)$$

This expression can be represented by the circuit of Fig. 5. Note that the capacitance is related to the maximum battery charge by  $C = Q_{max}/\mu$  and the parallel  $R_gC_g$  represents the first order HPF approximation, where  $R_g = \mu(n_1 - 1)/d_0Q_{max}$  and  $C_g = Q_{max}/\mu(n_1 - 1)$ . Often, the series of  $E_0$  and the capacity,  $C$ , is replaced by the OCV. The circuit structure is called Thevenin Battery Model and can be extensively found in the literature (see for example Refs. [29,30] used for State of Charge estimation; also computational implementation costs with respect to higher order degree approximation were studied in Ref. [31]). It is noteworthy that the circuit is analog to our model, from battery current/potential point of view, only if the OCV is approximated by the series of a capacitance and a constant voltage source, which constitute a quasi-linear system, otherwise the nonlinearity of the OCV affects different in both models.

Other popular battery model used to represent the dynamics of the stored charge for design engineering applications is presented in Ref. [14]. It is a battery model based on the approach of chemical kinetics, known as *kinetic battery model* also known as the hydraulic model; and it is depicted in Fig. 6. Specifically, it takes into account the rate capacity effect by assuming that the charge can be stored in two ways, either as immediately available or as chemically bound. It is generally described by the analogy of two-tanks. The bound charge can be released at a rate proportional to a constant  $g$ . The total charge ( $Q_{max}$ ) in the battery at any time is the sum of both the immediately available ( $q_1$ ), and the chemically bound ( $q_2$ ). Considering that  $q_1$  and  $q_2$  are the tank levels of areas  $\beta$  and  $1 - \beta$  respectively, the equations describing the charge dynamics are given by

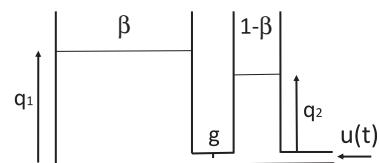


Fig. 6. Equivalent hydraulic model or kinetic battery model.

$$\beta \dot{q}_1(t) = (q_2(t) - q_1(t))g, \tag{40}$$

$$(1 - \beta) \dot{q}_2(t) = (q_1(t) - q_2(t))g + u(t), \tag{41}$$

where  $\beta \in [0,1]$  is the ratio of available charge capacity to total capacity and  $g$  is a rate constant in 1/time. By performing the following change of coordinates:

$$\text{SOC} = \beta q_1 + (1 - \beta)q_2, \tag{42}$$

$$X = q_2, \tag{43}$$

the following equations succeed:

$$\begin{pmatrix} \dot{\text{SOC}}(t) \\ \dot{X}(t) \end{pmatrix} = \begin{pmatrix} 0 & 0 \\ \frac{g}{\beta(1-\beta)} & -\frac{g}{\beta(1-\beta)} \end{pmatrix} \begin{pmatrix} \text{SOC}(t) \\ X(t) \end{pmatrix} + \begin{pmatrix} 1 \\ \frac{1}{1-\beta} \end{pmatrix} u(t) \tag{44}$$

which is equal to equation (36) with the equivalences  $d_0 = g/\beta(1 - \beta)$ ,  $n_1 = 1/(1 - \beta)$ , and  $u = I_{\text{bat}}/Q_{\text{max}}$ . Note that  $n_1$  is lesser than one, as it is expected according to the characteristic of the HPF. Note that this dynamic is equal to the linear second order approximation (36) of our general model. This dynamical part of the model needs to be completed with the battery voltage model. A voltage model given by  $E_{\text{bat}} = E_0 + k_1p + k_2p/(k_3 + p) + r_{\text{eq}}I_{\text{bat}}$  was proposed, where  $k_1, k_2, k_3$  are constants, and  $p$  is the normalized charge removed from the battery that is obtained from the discharge data, as explained in Ref. [27]. Sometimes, other voltage models are used, such that the Unwehnr Universal Model [28] expressed by  $E_{\text{bat}} = E_0 - k\text{SOC} + r_{\text{eq}}I_{\text{bat}}$ , where  $k$  is a constant. However, in all these cases the voltage model is different from equation (34), since

we used  $X$  instead of SOC, which is electrochemically correct. Thus, with this model approach, the RCE model corresponds with our second order model approximation, but the voltage model is built using tables which is not practical for BMS applications. Others voltages models uses SOC instead of  $X$  which does not represent the real electrochemical relationship, as it is described with our model, leading to erroneous results.

#### 4.2. Saturation and hysteresis

For the complete model, the effect of the saturation concentration  $X$  and the hysteresis remains to be included. To this end, we consider that the concentration saturation at the interface affects the charge current in the sense that when  $X$  is equal to one/zero, only a fraction of the charge current can be accumulated/delivered. In such circumstances the assumption that the charge current is approx equal to the battery terminals is not fulfilled. In order to obtain such current, the following algorithm is used:

$$\begin{aligned} &\text{if } X > 1 \text{ and } I_{\text{bat}} > 0, \text{ then } I = \max(I_{\text{bat}} - \lambda(X - 1), 0); \\ &\text{else, if } X < 0 \text{ and } I_{\text{bat}} < 0, \text{ then } I = \min(I_{\text{bat}} - \lambda X, 0) \\ &\text{else, } I = I_{\text{bat}}; \text{ end; end;} \end{aligned} \tag{45}$$

where  $I_{\text{bat}}$  is the battery current and  $\lambda$  is a positive constant high value. This algorithm takes a proportion of the load current, so that the concentration  $X$  does not deviate from values close to saturation. Common values of  $\lambda$  range from 20 to 40.

The hysteresis problem arises from the fact that the EMF in the charge is different from that obtained in the discharge. In certain batteries this phenomenon is significant and must be taken into consideration. Assuming  $f_E^c(0, X)$  and  $f_E^d(0, X)$  are the charge and discharge of EMF, the following algorithm was used in our model:

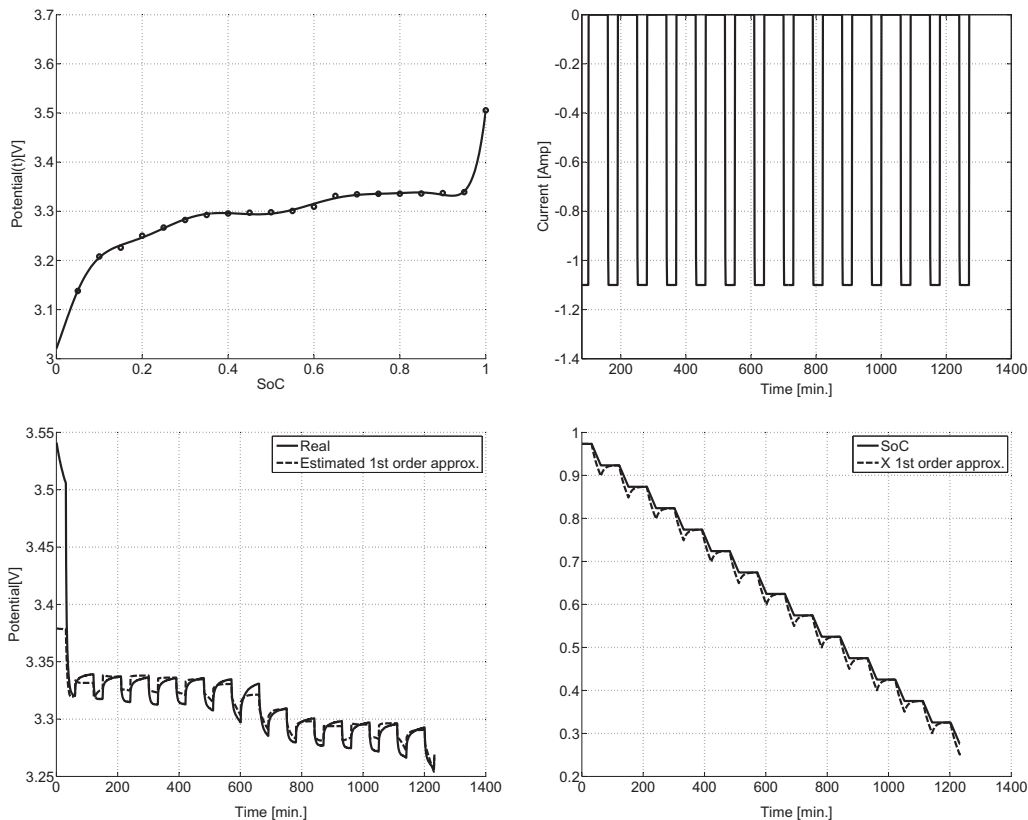


Fig. 7. Experiment 1. Lithium ion, 10 Ah.

$$f_E(0, X(k)) = p(k)f_E^c(0, X(k)) + (1 - p(k))f_E^d(0, X(k)), \quad (46)$$

$$p(k) = \lambda p(k - 1) + (1 - \lambda)sg(I_{bat}(k)), \quad (47)$$

where  $sg(I_{bat}(k))$  is one if the sign of  $I_{bat}(k)$  is positive, and zero if it is negative. The forgetting factor  $\lambda$  is within the interval  $[0,1]$  and weighs the velocity of change between both EMF functions.

**5. Results**

In this section we present the identification of the model parameters, as well as the model performance. We consider the second order approximation of equation model (36) with the voltage model given by the approximation in equation (35). The saturation and hysteresis are also considered. The model parameters to be identified are  $Q_{max}$ ,  $d_0$ ,  $n_1$ , and  $r_{eq}$ . To this end, the continuous-time model (31) is discretized using a sampling period  $h = 60\text{seg}$  and approximating the derivative by the backward shift approximation,  $dx(t)/dt \approx (x(kh) - x(kh - h))/h$ , giving the following discrete-time model:

$$X(k + 1) = \Phi_d X(k) + \Gamma_{1d} SOC(k) + \Gamma_{2d} I_{bat}(k) + \chi(k), \quad (48)$$

where  $\Phi_d = (1 - hd_0)$ ,  $\Gamma_{1d} = hd_0$ , and  $\Gamma_{2d} = hn_1/Q_{max}$ . The discretized voltage model is given by

$$E_{bat}(k) = f_E(0, X(k)) + r_{eq} I_{bat}(k). \quad (49)$$

First, the value of  $r_{eq}$  is obtained. Taking into account equation (48), the resistance  $r_{eq}$  can be obtained for fast variations of potential due to increments of current, as follows:

$$r_{eq} \approx \frac{1}{N} \sum_{k=1}^N \frac{E_{bat}(k) - E_{bat}(k - 1)}{I_{bat}(k) - I_{bat}(k - 1)}; \quad \text{for } |I_{bat}(k) - I_{bat}(k - 1)| > \varepsilon \quad (50)$$

where  $N$  is the number of current steps and  $\varepsilon$  is a threshold. Using this equation, the calculated internal resistance is an averaged value. In order to identify the parameters  $d_0$  and  $n_1$ , we first obtain  $X$  from the voltage error and the inverse of the EMF, as follows:

$$X(k) = f_X(0, E_{bat}(k) - r_{eq} I_{bat}(k)). \quad (51)$$

In the case where the EMF has hysteresis, an intermediate value from charge/discharge values was considered for obtaining  $X(k)$ . By assuming that the value of  $Q_{max}$  has been previously identified and that the disturbances  $\chi(k)$  are small with respect to the states, using the experimental values of  $I_{bat}(k)$  and  $SOC(k)$  together with the estimated values of  $X(k)$ , the coefficients  $d_0$  and  $n_1$  can be identified by using equation (48). The problem leads to the following linear regression model:

$$X(k) - X(k - 1) = hd_0(S(k - 1) - X(k - 1)) + \frac{hn_1}{Q_{max}} I_{bat}(k - 1). \quad (52)$$

In order to obtain the voltage/current register for parameter identification, we propose performing two tests. On one side, starting with a full-charge battery, a train of regular discharge pulses of current is used to determine the capacity  $Q_{max}$ . Also, the SOC is obtained. Assume, as well, that the pulses are enough spaced in time so that the system relaxes between pulses. Taking into

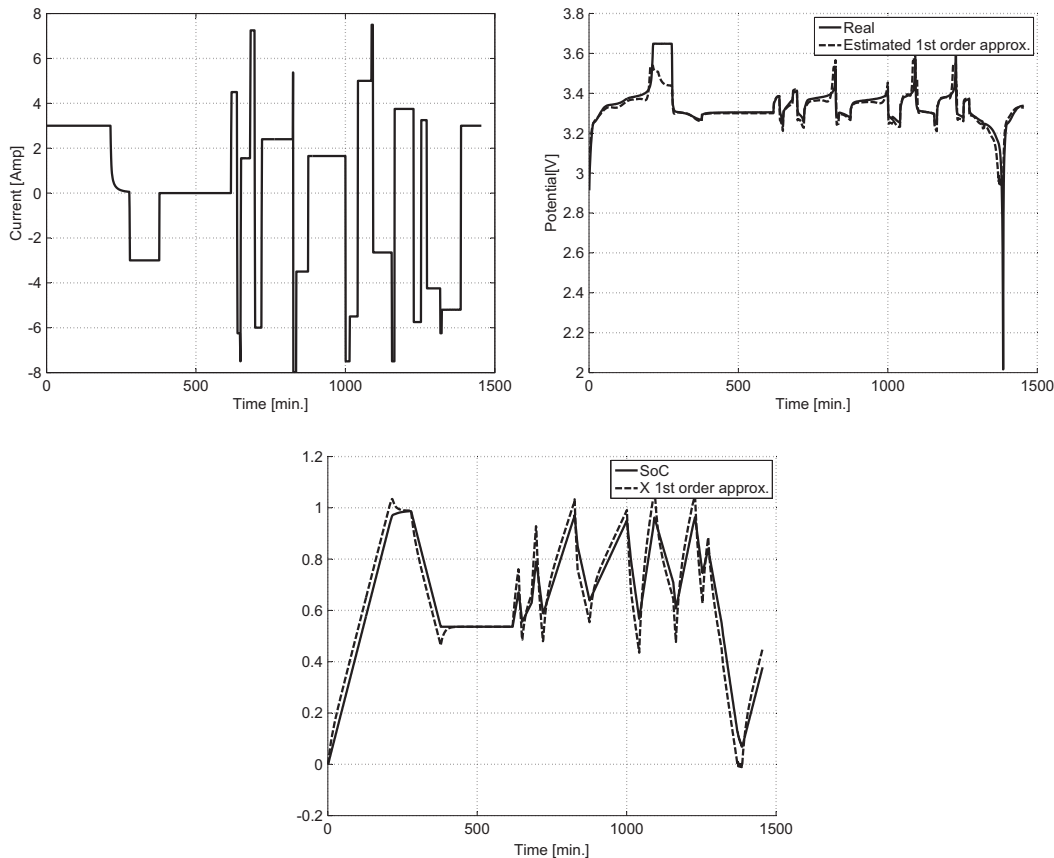


Fig. 8. Experiment 2. Lithium ion, 10 Ah.

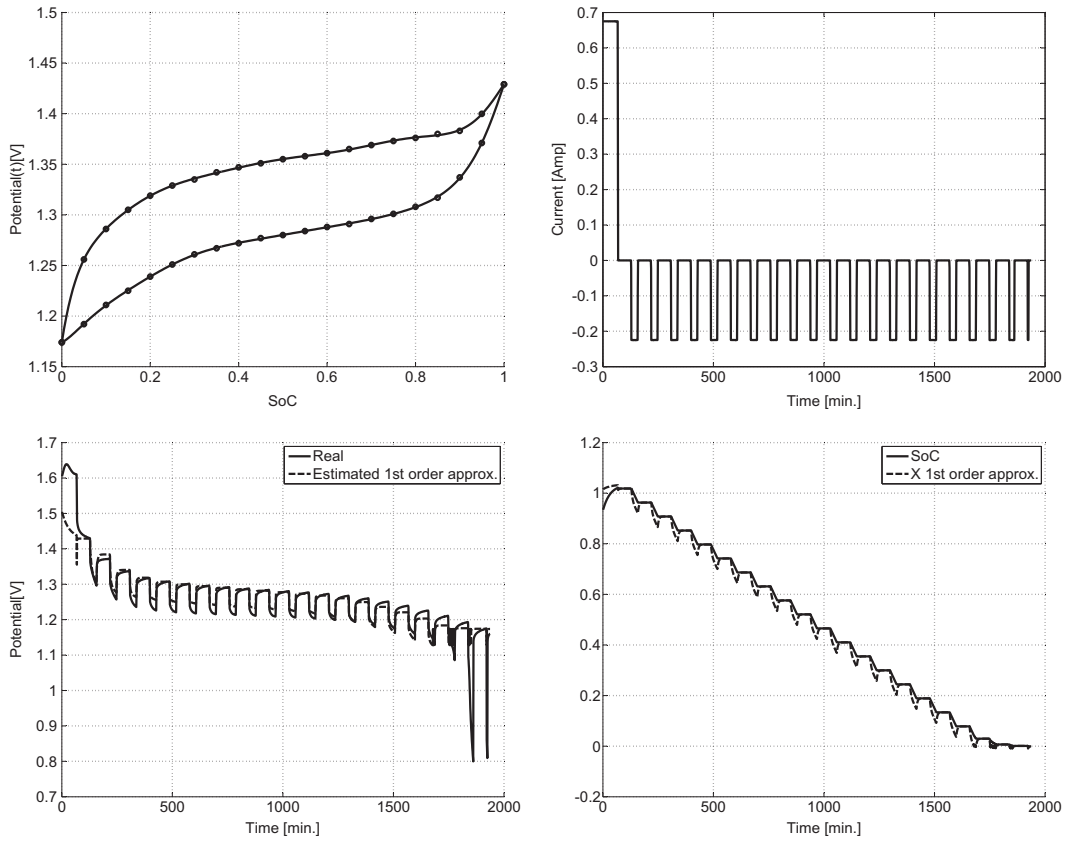


Fig. 9. Experiment 1. NiMH, Sanyo 2.7 Ah.

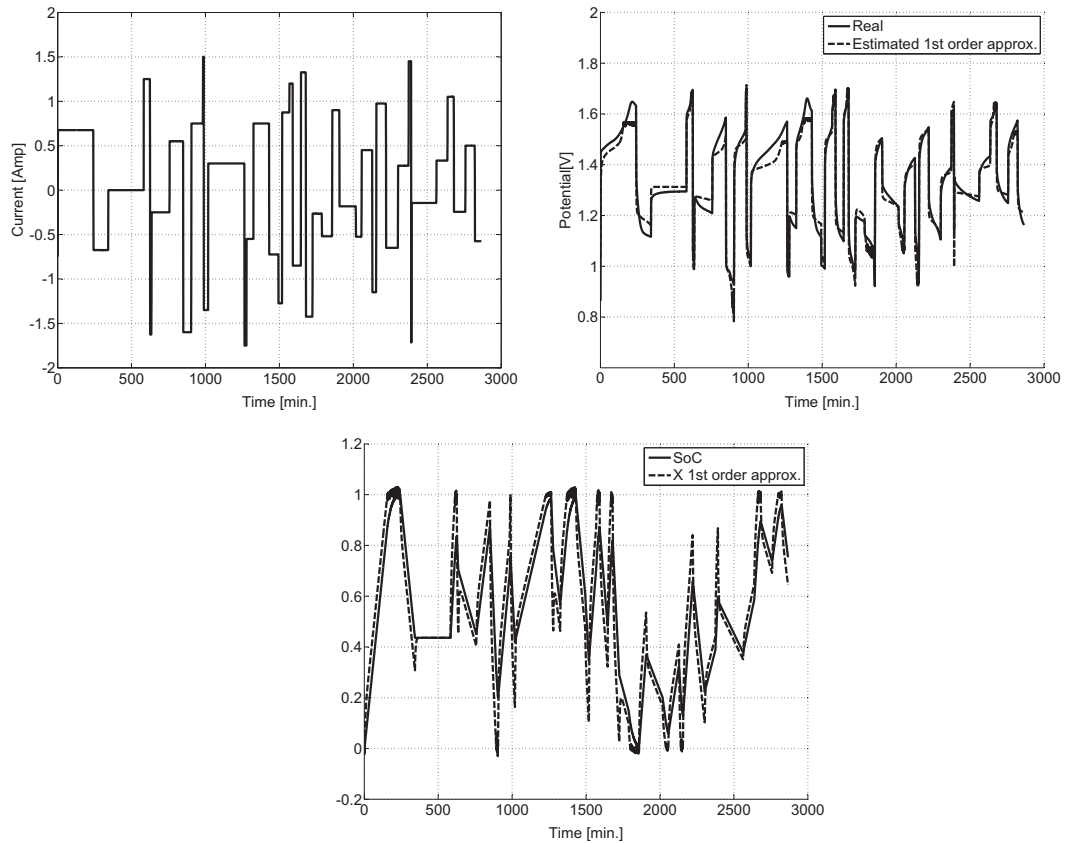


Fig. 10. Experiment 2. NiMH, Sanyo 2.7 Ah.

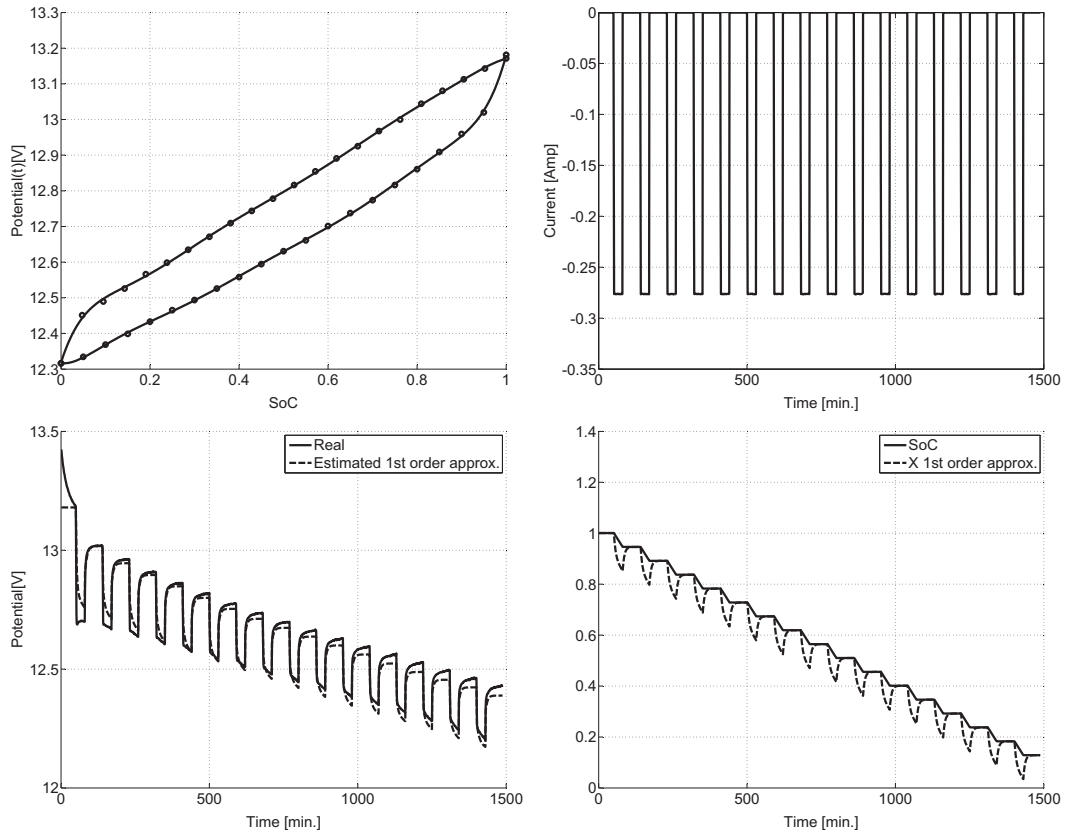


Fig. 11. Experiment 1. Lead acid, 7.5 Ah.

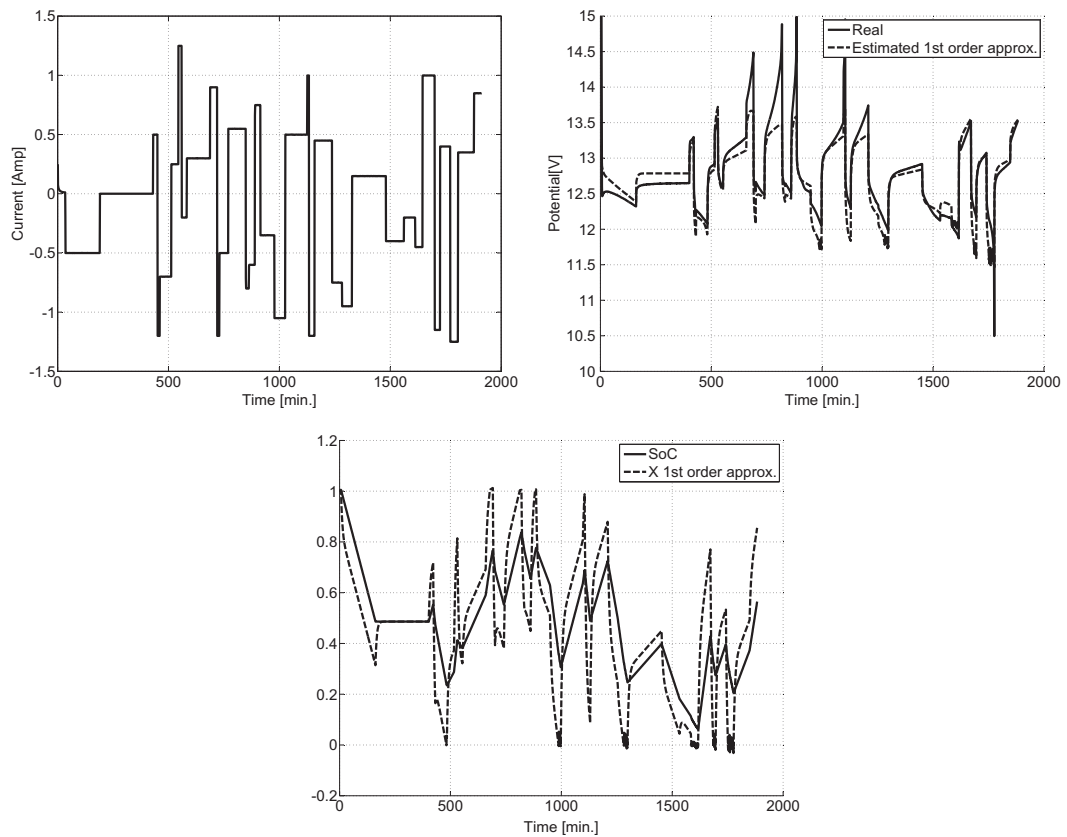


Fig. 12. Experiment 2. Lead acid, 7.5 Ah.

**Table 1**  
Identified parameters.

| Type | $d_0$ [s <sup>-1</sup> ] | $r_e$ [Ohms]          | $n_1$ [s <sup>-1</sup> ] | $Q_{max}$ [Ah] |
|------|--------------------------|-----------------------|--------------------------|----------------|
| Li   | $2.28 \times 10^{-3}$    | $1.13 \times 10^{-2}$ | 2.66                     | 11             |
| NiMH | $3.42 \times 10^{-3}$    | $2.05 \times 10^{-1}$ | 5.67                     | 2              |
| Pb   | $2.62 \times 10^{-3}$    | $5.5 \times 10^{-1}$  | 9.11                     | 2.5            |

account that after the system relaxes, the value of  $X$  is equal to the SOC, the EMF function is obtained by the pair (SOC, $E$ ) measured at the end of the relaxing time for each pulse. In order to identify the hysteresis, the same procedure is done for charge pulses to obtain a second EMF.

A second test is performed by using a random sequence of current pulses of different amplitudes and duration in both charge and discharge. This experiment is used to identify the constants  $d_0$ , and  $n_1$  using equation (52).

To achieve the initial state of charge, SOC = 0, a discharge current of small amplitude is applied until the potential decreases abruptly. Since the current is small, there is no voltage drop across the internal resistance. Consequently, the potential variation is solely due to the variation of surface concentration in the nonlinear region, where the value of  $X$  is approximately zero. A similar procedure is used to obtain SOC = 1.

In Figs. 7 and 8 both experiments are shown on a Lithium ion, TM SEIDEN, Mode: Prismatic LiFePO<sub>4</sub>E = 3.5 V, nominal capacity,  $Q_{max} = 10$  Ah battery. In Figs. 9 and 10, the same procedure was used for a Ni-MH, TM SANYO, Model HR-4UE = 1.2 V battery of nominal capacity  $Q = 2.7$  Ah; and in Figs. 11 and 12, the same procedure was applied to a Lead acid battery, TM Press, Model PR1240, E = 12 V with  $Q = 4$  Ah of nominal capacity. The parameter set obtained for the three batteries is shown in Table 1. Experiments have been performed with current values lower than 1C. Presumably, the resistance values do not vary significantly when higher current is applied. Should this not occur, a new parameter identification at high currents is suggested.

It is interesting to analyze the differences of the RCE among the three batteries tested. Solving equation (36) for a constant discharge current entry,  $I = -mQ_{max}$ , where  $m$  is an integer in units (1/time), the states SOC( $t$ ) and  $X(t)$  can be obtained. By performing the subtraction of the two states, the loss of capacity due to the RCE is obtained as

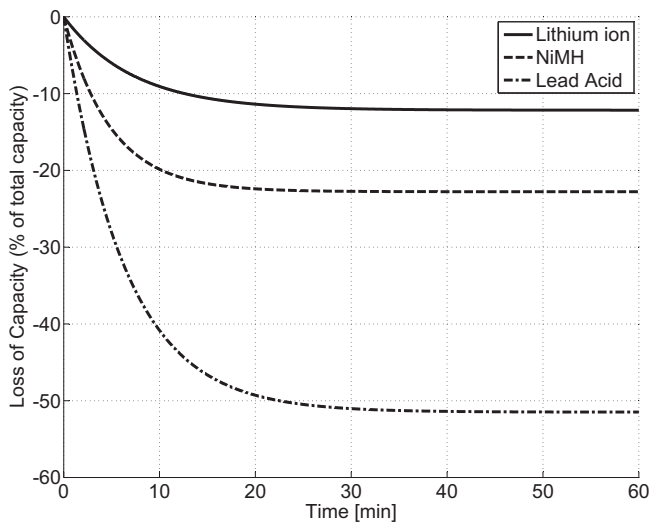


**Fig. 13.** Rate capacity for the three types of batteries.

$$SOC(t) - X(t) = m \frac{n_1 - 1}{d_0} (1 - e^{-d_0 t}). \tag{53}$$

It can be seen from the equation that the parameters  $d_0$  and  $n_1$  of the HPF define the RCE. In Fig. 13 the capacity lost due to RCE of all the batteries tested is depicted for constant current with  $m = 1 \text{ h}^{-1}$ . It can be seen that the Lithium battery has less RCE than Ni-MH, and it can also be seen that the lead acid battery shows a great RCE effect.

**6. Conclusions**

A simple model based on an electrochemical approach to be used in applications BMS has been presented. The key feature is that it can be used for any type of battery that works for charge accumulation and transport of matter. The model is based on two fundamental electrochemical states as the state of charge and the surface concentration. The latter is responsible for the RCE and enables a clear understanding of potential variation as a function of the surface concentration  $X$ . Tests show that a low-order approximation is indeed sufficient to obtain a good model. Furthermore, we have analyzed the similarities and differences with respect to other widely used simple models, demonstrating that our model has the same degree of simplicity associated with important electrochemical variables, which expands its range of use.

**Acknowledgments**

This work was supported by the Consejo Nacional de Investigaciones Científicas y Técnicas (CONICET), Agencia Nacional de Promoción Científica y Técnica, Universidad Nacional del Comahue and Universidad Nacional de La Plata; all of República Argentina.

**Appendix A**

The inverse function  $E = f_E(I, X)$  of equation (5) exists. In order to show this, let us state that a continuous function  $f$  is one to one if and only if it is either strictly increasing or decreasing with no local maxima or minima. In our case, the partial derivative with respect to  $E$  after some algebraical manipulation can be written as

$$\frac{\partial X}{\partial E} = \frac{k^o b \alpha^o e^{\alpha^o E} (1 - X) - k^r \alpha^r e^{\alpha^r E} X}{k^r e^{\alpha^r E} + k^o e^{\alpha^o E}}. \tag{54}$$

Taking into account that  $X \in (0, 1)$ , and  $\alpha^r < 0$ ,  $\alpha^o > 0$ , the derivative above is always positive. Thus, for each value of  $I$ , the inverse function  $E = f_E(X, I)$  exists. Hence, there is only one value of  $E$  for each couple  $(X, I)$ .

**Appendix B**

By taking into account that  $S = \sigma + j\omega$  the infinite dimensional rational function  $H(S)$  can be written as

$$H(\sigma + j\omega) = B^T ((\sigma \mathcal{I} - A) + j\omega \mathcal{I})^{-1} \gamma B F. \tag{55}$$

Thus, when  $\omega = 0$ ,  $H(\sigma) = B^T (\sigma \mathcal{I} - A)^{-1} \gamma B F$ , which is real for all  $\sigma$ , the first condition is fulfilled. To prove the second condition, taking into account that  $F$  and  $\gamma$  are positive real constants, we find that  $H(\sigma \geq 0) \geq 0$  iff  $-A \geq 0$ . Thus, we need to show that  $-A$  is positive semidefinite, which is the same as proving that given an arbitrary row vector  $Z$  always fulfills that  $-ZAZ^T \geq 0$ . Note that each element  $k_{ij}$  appears in matrix  $A$  at positions  $(ij)$  and  $(ji)$  with a positive sign, and at  $(jj)$  and  $(ii)$  with a negative sign. Then, each

element  $k_{ij}$  appears multiplied by  $-(Z_i - Z_j)^2$ , which is always negative semidefinite for arbitrary values of  $Z_i$  and  $Z_j$ . Since the elements  $k_{ij}$  are positive, we conclude that the matrix  $-A$  is positive semidefinite and the second condition for PRF of  $H(S)$  fulfills.

### Appendix C

Assume the potential  $E$  of the Butler–Volmer equation in equation (4) is a sum of two components. One due to the EMF given by equation (6), which does not depend on the current, denoted as  $E_1 = f_E(0, X)$ , and the other which depends on the current  $I$ , called  $E_2$ . The functional relationship between  $E_2$  and the current can be obtained by replacing  $E$  in equation (4) which gives

$$I = \gamma \left( e^{\alpha^o E_2} - e^{\alpha^r E_2} \right), \quad (56)$$

where  $\gamma = k^o X e^{\alpha^o E_1} = k^r (1 - X) e^{\alpha^r E_1}$  come from the fact that  $E_1$  is defined for  $I = 0$  and  $E_2 = 0$ . Then, the voltage equation (34) can now be written as follows:

$$E_{\text{bat}} = f_E(0, X) + (E_2 + r_e I_{\text{bat}}), \quad (57)$$

The second term on the right can be interpreted as the ohmic drop produced by an equivalent resistance  $r_{\text{eq}}(\gamma, E_2)$  given by

$$r_{\text{eq}}(\gamma, E_2) = \frac{E_2}{I_{\text{bat}}} + r_e \quad (58)$$

Now, we want to know the dependency of  $r_{\text{eq}}(\gamma, E_2)$  with both current and concentration. To this end, note that the symmetry factor of electrodes in a rechargeable battery has a value approximately equal to  $\alpha^o = 0.5$ . This means that the charge current corresponding to positive overpotentials are approximately the same than for discharge current corresponding to negative overpotentials. Then, the equality  $\alpha^o = -\alpha^r$  holds in equation (56) and the current can be written as

$$I = 2\gamma \sinh(\alpha^o E_2), \quad (59)$$

Thus, by assuming  $I_{\text{bat}} \approx I$ , the nonlinear resistance is given by

$$\frac{E_2}{I} = \frac{1}{2\gamma\alpha^o} \frac{\sinh^{-1}(I/2\gamma)}{I/2\gamma}. \quad (60)$$

It must first be noted that the element  $\sinh^{-1}(x)/x$  is a symmetrical decreasing function with a maximum value equal to one, at  $x = 0$ . Thus, the nonlinear resistance has its maximum value equal

to  $1/2\gamma\alpha^o$  at  $I = 0$ . As the current increases the resistance decreases. It is also worth mentioning that the constant  $\gamma$  increases with battery capacity as may be inferred from equation (56). Then, it is expected that for large capacity batteries the non-linear distortion is less significant. Finally, it is easy to see from equation (60) that for any given value of current amplitude, the nonlinear resistance decreases as  $\gamma$ - or equivalently  $X$ -increases.

### References

- [1] G. Ning, B.N. Popov, J. Electrochem. Soc. 151 (10) (2004) A1584.
- [2] V.R. Subramanian, J.A. Ritter, R.E. White, J. Electrochem. Soc. 148 (11) (2001) E444–E449.
- [3] O. Barbarisi, R. Caneletti, L. Glielmo, M. Gosso, F. Vasca, in: Proceedings of the IEEE Conference on Decision and Control, Las Vegas Nevada USA, 2002, pp. 1739–1744.
- [4] R. Milocco, B. Castro, J. Power Sources 194 (2009) 558–567.
- [5] K.A. Smith, C.D. Rahn, C.-Y. Wang, Energy Convers. Manage. 48 (2007) 2565–2578.
- [6] J. Lee, A. Chemistruck, G. Plett, J. Power Sources 206 (2012) 367–377.
- [7] X. Hu, S. Stanton, L. Cai, R. White, J. Power Sources 218 (2012) 212–220.
- [8] H.L. Chan, D. Sutanto, in: IEEE Power Engineering Society Winter Meeting, vol. 1, 2000, pp. 470–475.
- [9] B. Powell, T. Pilutti, Ford Scientific Research TR SR-93-201, December 1993.
- [10] Il-Song Kim, Trans. Power Electron. IEEE 23 (2008) 2027–2034.
- [11] S. Pang, J. Farrell, J. Du, M. Barth, in: Proceedings of the American Control Conference, 2, 2001, pp. 1644–1649.
- [12] J. Chiasson, B. Vairamohan, in: Proceedings of American Control Conference, Denver, CO, 2003, pp. 2863–2868.
- [13] B.S. Bhangu (Member, IEEE), P. Bentley, D.A. Stone, C.M. Bingham, IEEE Trans. Veh. Tech. 54 (3) (2005) 783–794.
- [14] J.F. Manwell, J.G. McGowan, Solar Energy 50 (5) (1993) 399–405.
- [15] M. Doyle, J.S. Newman, J. Appl. Electrochem. 27 (7) (1997) 846–856.
- [16] T. Wang, C.G. Cassandras, Automatica 48 (2012) 1658–1666.
- [17] J. Newman, W. Tiedemann, AIChE J. 21 (1) (1975) 25.
- [18] B. Paxton, J. Newman, J. Electrochem. Soc. 144 (1997) 3818–3831.
- [19] H.A. Kiehne (Ed.), Battery Technology Handbook, second ed., 2003.
- [20] P. De Vidts, R.E. White, J. Electrochem. Soc. 142 (1995) 1509–1519.
- [21] Omar Wing, Classical Circuit Theory, Springer Science, NYI, 2008.
- [22] T. Jacobsen, K. West, Electrochim. Acta 40 (2) (1995) 255–262.
- [23] T. Wigren, Thesis, Uppsala University, 1990.
- [24] J.C. Gómez, Baeyens, Lat. Am. Appl. Res. 33 (4) (2003) 449–456.
- [25] L.E. Unnewehr, S.A. Naser, Electric Vehicle Technology, John Wiley and Sons, New York, NY, 1982.
- [26] J.F. Manwell, J.G. McGowan, in: Proceedings of the 5th European Wind Energy Association Conference (EWEC '94), 1994, pp. 284–289.
- [27] H. Laig-Horstebrock, E. Meissner, G. Richter, US Patent and Trademark Office, Patent 6362598, Mar. 26, 2002.
- [28] Shuoqin Wang, Mark Verbrugge, John S. Wang, Ping Liu, J. Power Sources 196 (20) (2011) 8735–8741.
- [29] Hanlei Zhang, Mo-Yuen Chow, in: Proceedings of IEEE Power and Energy Society General Meeting, Minneapolis, Minnesota, USA, July 25–29, 2010.
- [30] Thomas Kailath, Linear Systems, in: Prentice-Hall Information and System Science Series, 1979.
- [31] L. Ljung, T. Söderström, Theory and Practice of Recursive Identification, MIT Press, 1983.